C. Wang et al. (Eds.)

doi:10.3233/ATDE230311

Multi-Objective Optimization Study of Dual-Fuel Engine Emissions and Economy

Cheng MA[a,b], Jie LI[b], Lixin PANG[b] and Jianyuan FENG[b,c,1]
[a] *Ocean Science and Engineering, South China University of Technology, Guangzhou, Guangdong, China*
[b] *APT Mobile SATCOM Limited, Shenzhen, Guangdong, China*
[c] *Peng Cheng Laboratory, Shenzhen, Guangdong, China*

Abstract. In the multi-objective performance optimization process for dual-fuel engines, the conflict between emissions and fuel efficiency is a consideration. To find a satisfactory compromise among many optimal solutions, reduce the difficulty of selecting solutions, and respond to different needs, a decision-making preference optimization strategy is introduced. The reliability prediction algorithm of the micro-ignition diesel/natural gas (NG) dual-fuel engine is built using support vector machines (SVM). The performance prediction model is combined with the optimization algorithm, and the preference information of the decision-maker (DM) is introduced into the optimization process, to guide the population evolution process to the direction that the DM is interested in, and achieve multi-objective preference optimization. Selecting nitrogen oxide (NO_x) emission and braking specific fuel consumption rate (BSFC) as the optimization targets, the optimal Pareto front surface is obtained. It can be seen from the simulation results that after introducing the decision preference, the evolution of the population can proceed in the direction of interest to the DM. Preference optimization can be achieved by rationally configuring the preference strength parameter δ, the weight vector w, and the reference point g. The combination of control parameters corresponding to the two preferences was downloaded to the ECU for bench test, and compared with the original data, it was found that when low emissions are preferred, the NO_x emission meets the IMO Tier-III limit under all working conditions, and the average NO_x emission is $1.22 g\cdot(kW\cdot h)^{-1}$, which is 78.9% lower than the original engine. At the same time, it was found that even with lower emissions, fuel consumption was reduced by 4.94% compared to the original engine. The preference for lower fuel consumption is 3.68% lower than the preference for lower emissions, but the deterioration of NO_x emissions is obvious.

Keywords. Preference decision-driven, multi-objective optimization, dual-fuel engine, performance optimization

1. Introduction

In response to the clash between the aim of high economy and thermal efficiency and the growth in emissions, engine management and conservation of energy and decreased emissions solutions are currently created. As a result, numerous studies have been conducted to optimize fuel injection strategy, adopt new combustion technologies, adopt alternative fuels, and add after-treatment equipment in order to meet the aim of energy

[1] Corresponding Author, Jianyuan FENG, APT Mobile SATCOM Limited; Peng Cheng Laboratory, Shenzhen, Guangdong, China; Email: jyfeng@apsat.com.

savings and pollution reduction. Due to its inherent low cost and plentiful supplies, compressed NG has caught the interest of researchers within the current energy mix [1]. However, using NG results in higher levels of unburned hydrocarbons and carbon monoxide. High productivity and minimal emissions, and an equilibrium between hydrocarbons and nitrogen oxides may all be attained by improving the engine's combustion chamber's structural layout, the fuel injection parameters, and the lean combustion conditions [2]. As the injection pressure rises, the rate at which methane flames propagate and the suggested thermal efficiency both rise, according to Chen's research of the impact of injection pressure on the operation and emissions of a dual fuel engine [2]. However, this causes an increase in total hydrocarbon emissions as the methane remaining in the cylinder wall gap cannot be ignited. Wu et al. [3] indicated that the pilot fuel injection timing and pressure are crucial parameters to achieve efficient and clean combustion at fixed operating conditions. The performance of dual-fuel engines was examined by Yousefi et al. [4] who discovered that advanced injection time would boost peak cylinder pressure, thermal efficiency, and NOx emissions throughout the entire operating condition range. They also went into great detail about how the primed diesel injection strategy affects engine performance and emissions at low loads and mentioned how using a twice-injected primed fuel strategy can help lower peak cylinder pressure and achieve a balance between NOx and CO and NOx and CH4. The study analysis discussed above demonstrates that the ignition fuel injection parameters have a significant influence on the property of dual fuel engines, choosing an appropriate arrange for the pilot fuel injection parameters is critical for addressing the high efficiency and low emission of dual fuel engines.

Furthermore, researchers discuss the influence of NG substitution rate (SR) on the nature of dual-fuel engines [5]. Although higher SR can reduce NOx emissions, they can increase HC emissions. The border of the SR is constraint on the engine thermal load. Chon et al. [6] investigated the impact of different air-fuel ratio (AFR) on engine performance and obtained an equilibrium between fuel consumption (BSFC) and NOx emissions by optimizing the AFR and injection parameters. It is not difficult to find what when designing controllers, it is necessary to obtain the optimal combination of control parameters to reduce pollution emissions under different operating conditions and improve economy.

However, reconciling the conflict between emissions and fuel consumption in dual-fuel engines requires optimizing controllable parameters, which requires solving complex multi-objective optimization problems [7]. The NSGA-II method was employed in the literature [8] to optimize the injection parameters as well as the engine combustion chamber geometry. Discussion also included the impact of pilot fuel injection timing and pre-injected diesel mass on emission characteristics. The ideal design point for reducing both BSFC and NOx emissions was found by CHO et al. [6] using a Pareto optimization technique. Additionally, a number of other optimization techniques have been applied to enhance engine performance and emissions [9].

The full-service functioning of maritime dual-fuel engines still needs improvement, notwithstanding the relative thoroughness of earlier research. more specifically, existing studies have shown that multi-objective optimization techniques usually obtain a set of mutually exclusive optimal solutions widely distributed in the objective space. The DM, however, is typically more interested in a particular solution or a number of options rather than the overall Pareto optimum solution in practical applications. To meet the needs of practical applications, this study uses preference multi-objective optimization to solve the above problem. A stringent partial order set is constructed on the Pareto non-dominated solution set by adding preference information to the multi-objective optimization framework, which directs the algorithm search in the direction of the DM's preferred area. Pareto-optimal solutions are obtained along with solutions that are satisfactory to the DM. First, a support vector machine (SVM)-based engine performance prediction model is created using data from bench trials on the emissions and fuel consumption of dual-fuel engines. Then the prediction model is combined with an optimization algorithm to perform preference optimization of the engine parameters for full operating conditions. Finally, the obtained preference solution is compared with the optimal solution without preference driving. It is confirmed that the preference-driven optimization strategy is feasible.

2. Test

2.1. Dual-Fuel Engines

The test was conducted using a six-cylinder inline four-stroke engine that has a compressed NG intake system. Table 1 displays the engine's technological specs.

Table 1. The test engines' technical details.

Parameters	Value
Rated speed (r/min)	1500
Rated power (kW)	255
Max fuel injection pressure (bar)	1500
Number of cylinders & layout	6-inline
Compression ratio	16.5:1
Displacement (L)	12.155
Stroke (mm)	155
Bore (mm)	129

A 6-cylinder inline 4-stroke dual fuel engine fitted with a compressed NG delivery system was used for the experiments. To deliver the load, the flywheel end was attached to an eddy current dynamometer. To monitor the engine running condition and performance data, the test equipment included an ES636 meter, an E+H flow meter, an emission analyzer, and an AVL fuel consumption meter. The E+H flow meter is used to monitor the NG flow, in order to precisely define the engine economy index. The full experimental test bench's schematic diagram is shown in Figure 1. Table 2 displays the range and accuracy of all test instruments.

The low calorific value of NG is used to convert it to diesel use, and the mathematical calculation is as follows, in order to appropriately reflect the economic indicators of the dual-fuel engine.

$$m_{dual} = m_{diesel} + \frac{H_{u_{CNG}}}{H_{u_{diesel}}} \times m_{CNG} \tag{1}$$

$$\frac{H_{u_{CNG}}}{H_{u_{diesel}}} = 1.15 \tag{2}$$

where, H_μ indicates a low calorific value, ($J \cdot kg^{-1}$). The mass flow of the fuel is denoted by m, in ($kg \cdot h^{-1}$).

Table 2. Main equipment.

Equipment	Application		Range
AVL 736	Fuel consumption meter		0-125 kg/h
		NOx	0-10000
AVL AMA i60	Emission analysis	CO/CO_2	0-5000
		THC/CH_4	0-20000
PROMASS 83 A DN04/ 1/8’’	Air/Gas flow measurement		0-90 kg/h
Dynamometer	Load torque		0-320 kW
Magnetoelectric sensor	Engine speed		0-10000 r/min

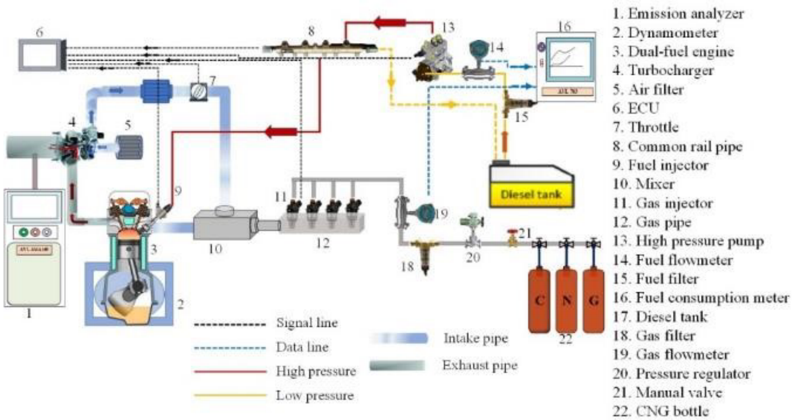

Figure 1. The experimental setup is illustrated graphically.

2.2. Input and Output Parameters and Ranges

A diesel/NG dual-fuel engine that uses diesel as the pilot fuel and the multiple injection control approach is the study subject of this work. The ratio of NG to diesel, or the replacement rate of the dual-fuel engine, must be considered in the modeling analysis of the dual-fuel engine in addition to the conventional performance parameters such as rail pressure, injection timing, and pre-injection volume, which have a significant impact on the engine performance. Better atomization can boost engine efficiency but raises in-cylinder temperature, which increases NOx emissions [10]. Fuel atomization is determined by the fuel system injection pressure. although the BSFC rises [11], postponing the main injection period can successfully reduce NOx emissions. Zhao et al. [12] found through experimental studies that NOx emissions are reduced with the advancement of pre-injection timing which is conducive to the optimization of emission and economy. Another study showed that proper pre-injection can effectively improve engine economy and reduce NOx emissions [13]. Wang et al. [14] showed that NOx emissions and BSFC decreased with increasing EAC, but when the EAC was too high, it was easy to cause misfire phenomenon; higher NG replacement rate led to lower maximum in-cylinder temperature and reduced NOx emissions, but the indicated power decreases and some economy is lost [15]. Additionally, a few earlier studies demonstrated the limited impact of control settings on emission and BSFC patterns [16].

Different operating points are determined according to engine speed and torque, and the best combination of control parameters under various operating points is determined by optimizing the remaining six control parameters. The input parameters of the support vector machine prediction model are set as follows: speed, torque, rail pressure, MIT, PIT, PIQ, EAC, and SR. NOx emission and BSFC are specified as the output parameters.

The boundaries of the input and output parameters need to be considered as follows:

(1) The lower limit of torque is determined according to the boundary of stable engine operation in dual fuel mode as 300 N·m, while the upper boundary is similar to that of diesel mode, which is the maximum torque corresponding to different speed, and the change of torque with speed is determined according to the external characteristic curve.

(2) The maximum value of the SR is limited by the amount of primed diesel fuel, which must be greater than the maximum pre-injection amount to ensure the smooth operation of the engine, and the maximum pre-injection amount is determined to be 9 (mg·cyc^{-1}) after several tests. therefore, the boundary range of the SR is shown in Figure 2, and the range of the remaining parameters is shown in Table 3.

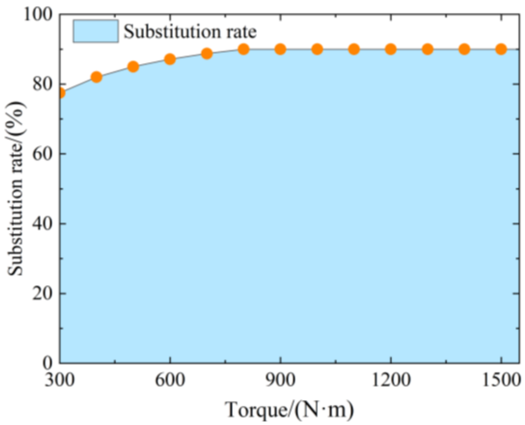

Figure 2. The range of substitution rate.

Table 3. Input parameters and ranges.

Speed	**MIT**	**PIT**	**PIQ**	**RP**	**EAC**
$(\mathrm{r\cdot min^{-1}})$	(°CA)	(°CA)	$(\mathrm{mg\cdot cyc^{-1}})$	(MPa)	_
800-1500	-2-6	50-70	2-6	60-100	1.4-1.9

In order to obtain the experimental data required for modeling while avoiding the increased costs associated with extensive testing, this study relies on V-optimization and space-filling experimental design methods for the condition point design [16-18]. The main injection time is utilized as a local input whereas the other parameters are used as global inputs since it has the largest impact on engine characteristics. To ensure the model's generalization capacity, the test points designed include 75 space-filling and 25 V-optimized design supplementary points, totaling 100 test points, by referring to Reference [16]. A total of 500 test points were employed to collect data on the engine test stand in accordance with the design operating conditions, together with the local inputs (MIT) [-2,0,2,4,6].

3. Performance Prediction Modeling Based on SVM

3.1. Introduction of SVM

Cortes and Vapnik first presented the Support Vector Machine (SVM) machine learning technique in 1995. It is based on the VC dimensional theory and the idea of structural risk reduction [19]. Vapnik created the insensitive loss function, whose fundamental concept is to locate the ideal classification hyperplane such that the error of all samples from that ideal classification plane is minimized, to solve the regression issue using support vector machines [20]. In order to address the nonlinear predictive regression issue, kernel functions are also utilized to translate nonlinear parameters to a feature space with high dimensions for linear regression.

3.2. Predictive Modeling

3.2.1. Parameter Normalization

Since the actual input parameters are of different orders of magnitude, in order to avoid the parameters of small order of magnitude being overshadowed by those of large order of magnitude, the input and output parameters are first normalized to between [-1,1]. The following is the mathematical expression:

$$\bar{x} = -1 + \frac{2\left(x - x_{\min}\right)}{x_{\max} - x_{\min}} \tag{3}$$

where: $x_{\max}$ is the sample maximum; $x_{\min}$ is the sample minimum; $\bar{x}$ is the normalized vector.

3.2.2. Kernel Functions

The prediction performance of support vector machine prediction models depends heavily on the penalty factor *C* and the choice of kernel function and its parameters. Because of its computational simplicity and strong prediction performance, the radial basis kernel function has been frequently employed in the research of engine performance prediction modeling. The radial basis kernel function is formulated as follows:

$$K\left(x_i, x\right) = \exp\left(-\frac{\left\|x - x_i\right\|^2}{2\sigma^2}\right) \tag{4}$$

3.2.3. Evaluation Indicators

The created performance prediction model's predictive capacity was estimate using the statistical measurement determination coefficient R^2, root mean square error (RMSE), and mean absolute error (MAE).

$$R^2 = 1 - \frac{\sum_{i=1}^{n}(f_i - y_i)^2}{\sum_{i=1}^{n}(y_i - \bar{y})^2} \tag{5}$$

$$RMSE = \sqrt{\frac{1}{n}\sum_{i=1}^{n}(f_i - y_i)^2} \tag{6}$$

$$MAE = \frac{1}{n}\sum_{i=1}^{n}|f_i - y_i| \tag{7}$$

where *n* is the length of the prediction series, f_i is value of the model prediction, y_i is measured value, and $\bar{y}$ is the mean of predicted values.

Structure of a SVM is shown in Figure 3.

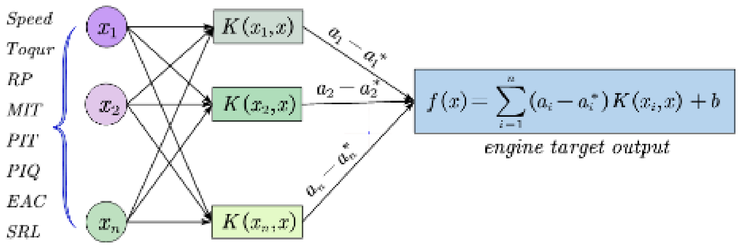

Figure 3. An SVM's structural diagram.

3.3. Prediction Results and Analysis

In order to find the optimal penalty factor *C* and kernel function radius *σ*, three different self-searching optimization algorithms are compared separately. Grid Search (GS) is the quickest way to find the ideal radius width of the radial basis kernel function and the penalty parameter C for the SVM model, but finding these parameters over a wide range takes a lot of time. when using heuristic algorithms for the optimization search, there is no need to traverse all parameter points in the grid, making it possible to find the global optimal solution more quickly [21]. The parameters of the SVM model's kernel function are improved using the GS method, PSO, and GA, respectively, to discover the best parameters and reduce computing time.

The support vector machine prediction model was trained using eighty percent of the experimentally gathered data, with the remaining twenty percent (non-participating training) being utilized as the test set to assess the model's predictive power. The effects of different search methods on the prediction accuracy of the 20% of data that did not participate in training are shown in Figure 4. It can be found out all three search methods can obtain good results, and the coefficients of determination R^2 of NO*x* and BSFC in the test set are between 0.97 and 1, indicating that the parameters obtained from the search can construct a support vector machine with excellent prediction performance.

Figure 5 compares the two methods, PSO and GA, in terms of how quickly they reach convergence. It is clear from the figure that the GA algorithm finds the optimal fitness value after 30 iterations, while PSO requires 100 iterations. Therefore, with the above considerations, the GA algorithm is chosen for the optimization search in this paper. As for the GS method, it is not used in this study because of the contradiction between the grid division size and the computation time and accuracy, which increases the design complexity.

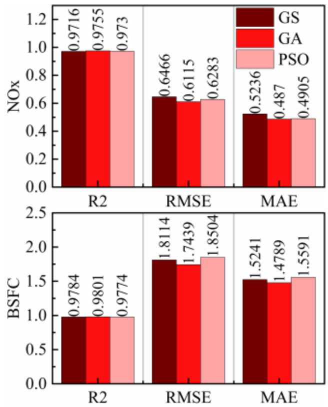

Figure 4. Comparison of different search methods.

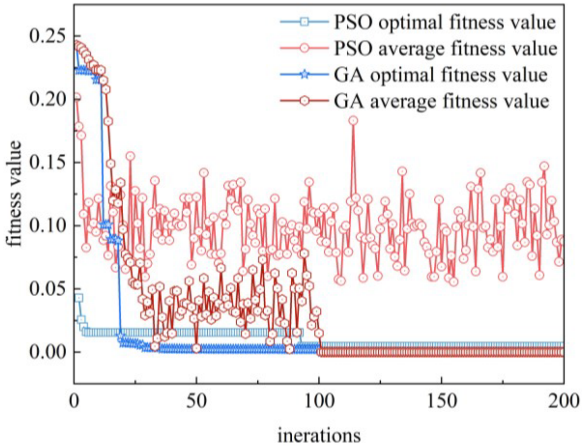

Figure 5. Comparison of convergence speed.

4. Preference-Driven Multi-objective Optimization

4.1. Definition

The priority that a DM accords to a certain area of the solution in the target space might be interpreted as preference. When the DM has some a priori knowledge and can directly give the importance of the goal (preference information), this type of preference is called deterministic preference. The preference relation reflects the DM's degree of need or preference between goals that have differences [22].

Interactive decision making, on the other hand, is a type of approach that adds preference information to the search process in an interactive manner. Since it is difficult for DMs without a priori knowledge to give precise preference information, the information carried by the solution set obtained by guiding the search with preference information is repeatedly fed back to the DM in the process of optimization through interaction, which guides the DM to continuously improve the preference information, so as to further guide the search of the algorithm and finally obtain a solution or solution set satisfactory to the DM. Concentrating the search of the algorithm in the preference region can effectively utilize the algorithm resources while reducing the computational complexity and improving the solution efficiency of the algorithm.

4.2. Multi-objective Optimization Algorithm Improvement

4.2.1. NSGA-II

The NSGA-II method not just implements an elite selection approach to prevent the eradication of the best people, but it also increases population diversity by allowing the genetic algorithm to search the whole solution space and discover the overall optimal solution. First, the two principles of non-dominated ranking and crowding distance calculation are used to evaluate the better individuals in each generation of the population; second, a fresh population of offspring is produced by mutation, crossover, and selection. Next, using the elite technique, the parent and offspring individuals of each generation are mixed, and the crowding distance and non-dominated ranking are calculated. Finally, the population is pruned according to the above two evaluation results, and this operation is performed indefinitely until the maximum number of iterations is achieved.

4.2.2. Preferred Information Introduction

- Basic Concepts

An optimization problem with numerous objective functions is referred to as a multi-objective optimization problem. The minimization issue with m objectives and n choice variables is taken into consideration without losing generality. The following is its mathematical definition:

$$\begin{cases} \min y = \boldsymbol{F}(x) = (f_1(x), f_2(x), \cdots, f_m(x))^T \\ l_i(x) \geq 0, i = 1, 2, \cdots, p \\ h_j(x) \geq 0, j = 1, 2, \cdots, q \end{cases} \tag{8}$$

where $x = (x_1, x_2, \cdots, x_n)^T \in \boldsymbol{X}$ is an n-dimensional decision variable, $\boldsymbol{X}$ is a decision space, $y = (y_1, y_2, \cdots, y_m)^T \in \boldsymbol{Y}$ is the goal to be optimized, and $l_i(x)$ and $h_j(x)$ are the optimization problem's constraints.

Lamjed Ben Said's proposal for a new dominance relationship combines the reference point strategy with the Pareto dominance relationship [23]. It is a solution that upholds the Pareto-induced order and is nearer the DM's frame of reference. The weighted Euclidean distance is used to determine if a solution in the solution set has reached convergence with the reference point [24].

$$Dist(x, g) = \sqrt{\sum_{i=1}^{M} w_i \left(\frac{f_i(x) - f_i(g)}{f_i^{\max} - f_i^{\min}} \right)^2} \quad w_i \in]0,1[, \sum_{i=1}^{M} w_i = 1 \tag{9}$$

where x is a potential solution, g is DM's reference point, and the i-th goal value's upper and lower bounds are represented, respectively, by $f_i^{\max}$ and $f_i^{\min}$. w_i is the i-th objective's weight vector.

- Definition (The r-Dominance Relation): Any two solutions in the feasible region, x and y, must be satisfied x r-dominance y only when one of the two conditions stated below is true:

(a) In the Pareto notion, x dominates y;

(b) Pareto does not dominate x and y, and $D(x,y,g) < -\delta$, where $\delta \in [0,1]$,

$$D(x,y,g) = \frac{Dist(x,g) - Dist(y,g)}{Dist_{\max} - Dist_{\min}} \tag{10}$$

$$Dist_{\max} = Max_{z \in P} Dist(z,g) \tag{11}$$

$$Dist_{\min} = Min_{z \in P} Dist(z,g) \tag{12}$$

where, also known as the preference intensity value, δ is a setting that controls the size of the preference region. $\boldsymbol{P}$ stands for the population as a whole, the population's greatest and minimum distances from the reference point are denoted by $Dist_{max}$ and $Dist_{min}$, respectively.

4.3. Problem Description

In order to solve the irreconcilable conflict between emission and fuel consumption of engines, this study takes NO*x* emission and fuel consumption rate BSFC as the optimization objectives. In the meantime, in order to satisfy the various requirements of various DM in response to various situations, the introduction of DM preference information guides the population's evolution and search, causing the effective computation to take place in the region of greater concern to DM and speeding up the algorithm's convergence to the preference region. Thus, the optimization results can directly meet the requirements of DMs.

$$\min \boldsymbol{F}(\boldsymbol{x}) = \left(f_1(\boldsymbol{x}), f_2(\boldsymbol{x})\right)^T \tag{13}$$

$$f_1(\boldsymbol{x}) = \mathrm{NO}x(\boldsymbol{x}) \tag{14}$$

$$f_2(\boldsymbol{x}) = \mathrm{BSFC}(\boldsymbol{x}) \tag{15}$$

$$g_1(\boldsymbol{x}) = \mathrm{THC}(\boldsymbol{x}) \le 0.9\mathrm{T}_{\mathrm{THC}} \tag{16}$$

$$g_2(\boldsymbol{x}) = \mathrm{CO}(\boldsymbol{x}) \le 0.9\mathrm{T}_{\mathrm{CO}} \tag{17}$$

$$\boldsymbol{x} = (\mathrm{RP, MIT, PIT, PTQ, EAC, SRL})^T \in D \tag{18}$$

where x is the decision vector made up of the control parameters, and Table 3 displays the range of values for each parameter. The emission regulation standard levels are $\mathrm{T}_{\mathrm{THC}}$ and T_{CO}; 0.9 is the safety factor; D is the decision space.

4.4. Optimization Results and Analysis

The effect of preference decision driving on the optimization results is illustrated in Table 4 for Case B as an example.

Table 4. Dual-fuel engine propulsion characteristics.

NO.	A	B	C	D	E	F	G	H
Speed	800	900	1000	1100	1200	1300	1400	1500
Torque	404	527	650	815	963	1128	1305	1510

4.4.1. Influence of Reference Points on Optimization Results

Figure 6 depicts the preferred Pareto-optimal solution set obtained by using three self-selected reference points as guides for the search to direct the population search direction. The optimization strength δ is set to be 0.5 for all, the population size is 50, the evolutionary generation is 200, and the $\boldsymbol{w}$=[0.5,0.5].

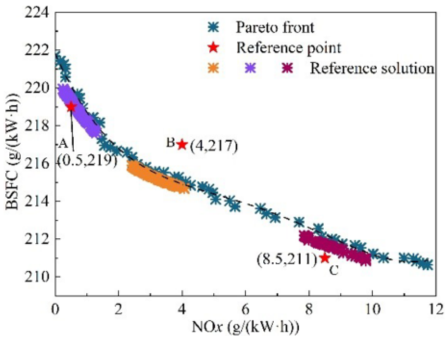

Figure 6. The effect of reference point selection on optimization outcomes.

From the figure, it can be found that for different reference points selected, the search results find the optimal solution closest to the true Pareto front. Moreover, whether the reference points are located inside the feasible domain [(0.5,218), (8.5,211)] or outside the feasible domain (4,217), they do not affect the solution search. It can be seen that the reference point is able to direct the search of the population towards the desired region.

4.4.2. Effect of Preference Strength on Results

Figure 7 compares the effect of different preference strength (δ=[1,0.8,0.5,0.2]) values on the obtained Pareto front solution distribution. The same reference point **R**=(4,210) and $\boldsymbol{w}$=[0.5,0.5], indicating that the DM has the same degree of preference for both objectives during the optimization process) are set in the experiment. When δ=1, the preference optimization algorithm obtains the entire Pareto frontier surface, indicating that the DM is interested in the entire set of frontier solutions at this time. As δ decreases, the range of the obtained solutions gradually decreases. Therefore, if the DM wants to obtain a larger range of the preferred solution set in the frontier solution set, he can choose a larger value of preference intensity, and vice versa. It can also be found that when the preference intensity value δ=1, the solution set is the same as the Pareto frontier solution set found by NSGA-II. The decrease of δ also indicates that the user is more interested in the pareto optimal solution close to the reference point, and it also helps the user to select the region of interest more directly without searching in the whole frontier plane.

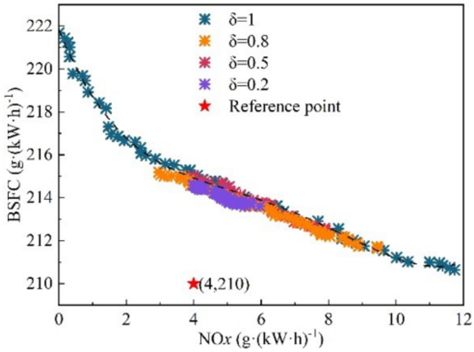

Figure 7. The impact of various preference strengths on the outcomes of optimization.

4.4.3. Effect of the **w** on the Results

The distribution of the optimization outcomes is examined in Figure 8 in relation to the weights of the weighted Euclidean distance. The values of the reference point and δ are set to (2.1,210) and 0.5 respectively. From the figure, it can be seen that changing the weight vector has an effect on the distribution of the preferred solutions. For the weight w=[0.5,0.5], the obtained preference solution lies in the middle of the entire Pareto front solution distribution. For the weight vector w=[0.8,0.2], the distribution of solutions shows that the optimization is carried out more focused on the objective f_1, i.e., the DM is more interested in reducing NOx emissions compared to BSFC. Similarly, for the weight vector w=[0.2,0.8], the DM wants to obtain a lower BSFC and thus needs to sacrifice some emission performance.

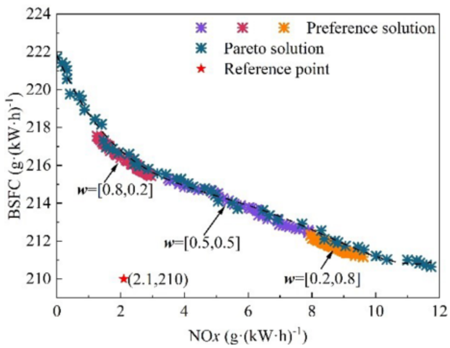

Figure 8. The influence of different weight vector on optimization results.

4.5. Experimental Test Results

The preceding discussion has demonstrated that using a preferred multi-objective optimization method can provide the Pareto optimum solution while causing a change in the distribution area of the solution of interest. Here, three operating conditions representing low, medium, and high loads (operating conditions B, E, and H) of engine operation are chosen for the analysis.

With low fuel consumption in area B, where NOx emissions exceed the maximum value (8.18 g(kWh)$^{-1}$), as specified in IMO Tier-II, and NOx emissions meeting the IMO

Tier-III regulation in area A, Figure 9 depicts the distribution of solutions corresponding to the various preferences for the three operating conditions. The settings of the preferred parameters for each operating condition are determined in an interactive optimization process. The DM prefers low emissions for w=[0.8,0.2], while the opposite preference for low fuel consumption for w=[0.2,0.8]. δ=0.3 than δ=0.5 indicates that the DM expects a smaller range of solution distribution.

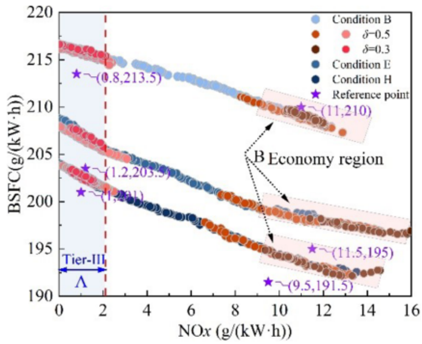

Figure 9. Distribution of solutions for different preference situations.

Preference optimization results for the full operating conditions are obtained by using an optimization process similar to the one described above. The solutions for each operating condition are randomly selected in regions A and B, and the MAP diagrams of all control parameters for the optimal solution are obtained using cubic polynomial interpolation. Figure 10 shows the MAP maps of the main injection timing for the two preferences. The MAPs of all control parameters were calibrated to the ECU for bench testing. The NOx emissions and BSFC are compared for the two preferred strategies.

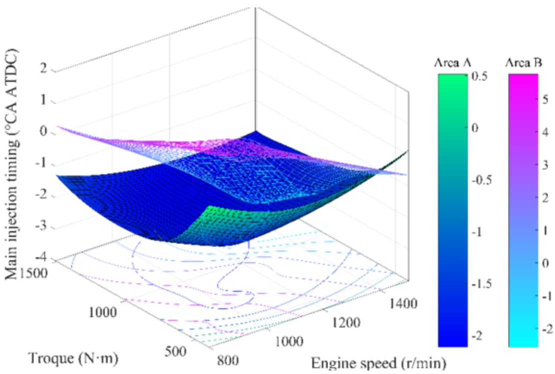

Figure 10. The main injection timing MAP corresponding to the two preferences.

Figure 11a shows that the NOx fulfills the IMO Tier-III standard of 2.08 g $(kW{\cdot}h)^{-1}$ across the whole operating range at the chosen low emission, with an average value that is 1.22 g $(kW{\cdot}h)^{-1}$, which is 78.9% lower than that of the original machine. Also in Figure 11b, it can be seen that the BSFC at the preferred low emission has also improved. This indicates that the optimization results in a simultaneous reduction of emissions and fuel consumption. Figure 11b shows that the BSFC achieved while choosing low fuel consumption is 3.68% lower than the BSFC obtained with low emissions and 8.44% lower than the original machine. However, the pursuit of lower fuel consumption comes at the cost of worsening emissions.

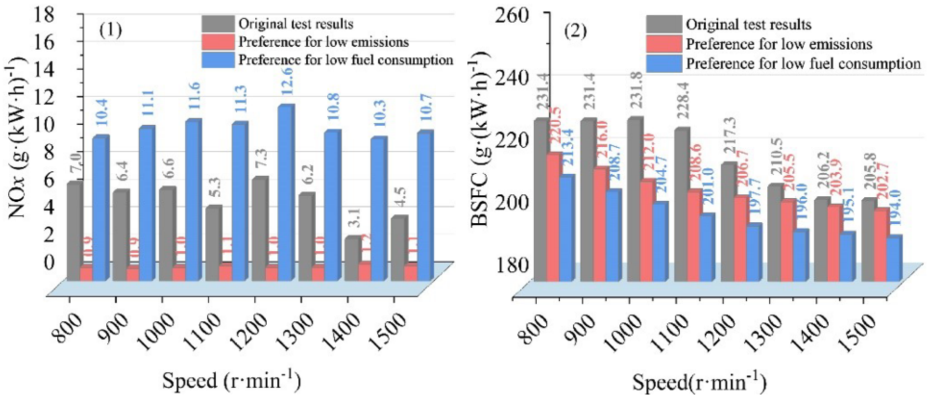

(a) (b)

Figure 11. The test results.

5. Conclusion

The SVM-based agent model used in this investigation, the test data show that the RMSE is less than 1.8 and the MAE is less than 1.5, indicating that the model has the ability to predict accurately and effectively. The effect of DM preference on the optimization outcomes is imaginatively taken into account together with the practical application requirements in the multi-objective optimization process. It is discussed how each preference parameter affects the distribution of the optimization outcomes. Any point in the feasible or infeasible domain, including the position of the reference point, reflects the ideal point envisaged by the DM. The DM's interest in a certain optimization objective can be taken into account when adjusting the $\boldsymbol{w}$ of the Euclidean distance. The range of the solution distribution has an inverse relationship with the magnitude of the preference strength value. Without having to worry about the absence of a priori information, the aforementioned parameters may be set during the interactive optimization process.

The optimization results under the two preference strategies are compared by an experimental bench. The preference for low emissions is to meet the specific requirements of emission regulations, and the preference for low fuel consumption is due to cost considerations. With an average NOx emission of 1.22 g·(kWh)$^{-1}$, which is 78.9% less than the original engine and significantly lower than the emission results obtained with preference for low fuel economy, the experimental results demonstrate that the solutions with a preference for low emissions all meet the IMO Tier-III requirements for NOx. There is no doubt that a preference for low BSFC leads to lower fuel consumption, and interestingly, in both states the BSFC is lower than the results obtained for the original engine. However, the higher fuel economy is obtained at the expense of damaging the environment.

Acknowledgements

This work was supported by the Shenzhen Science and Technology Plan Project (JSGG20220831100602005).

References

[1] Napolitano P, Fraioli V, Guido C, et al. Assessment of optimized calibrations in minimizing GHG emissions from a dual fuel NG/diesel automotive engine. Fuel. 2019;258:115997.1-115997.12.
[2] Chen Y, Zhu Z, Chen Y, et al. Study of injection pressure couple with EGR on combustion performance and emissions of natural gas-diesel dual-fuel engine. Fuel. 2020;261:116409.1-116409.12.
[3] Wu Z, Han Z. Micro-GA optimization analysis of the effect of diesel injection strategy on natural gas-diesel dual-fuel combustion. Fuel. 2020;259:116288.
[4] Yousefi A, Guo H, Birouk M. Effect of diesel injection timing on the combustion of natural gas/diesel dual-fuel engine at low-high load and low-high speed conditions. Fuel. 2019;235:838-846.
[5] Meng X, Tian H, Zhou Y, et al. Comparative study of pilot fuel property and intake air boost on combustion and performance in the CNG dual-fuel engine. Fuel. 2019;256:116003.1-116003.12.
[6] Cho J, Park S, Song S. The effects of the air-fuel ratio on a stationary diesel engine under dual-fuel conditions and multi-objective optimization. Energy. 2019;187:115884.1-115884.16.
[7] Lotfan S, Ghiasi RA, Fallah M, et al. ANN-based modeling and reducing dual-fuel engine's challenging emissions by multi-objective evolutionary algorithm NSGA-II. Applied Energy. 2016;175:91-99.
[8] Liu J, Zhao H, Wang J, et al. Optimization of the injection parameters of a diesel/natural gas dual fuel engine with multi-objective evolutionary algorithms. Applied Thermal Engineering. 2018;150:70-79.
[9] Sumit Roy RB. Multi-objective optimization of the performance-emission trade-off characteristics of a CRDI coupled CNG diesel dual-fuel operation: A GEP meta-model assisted MOGA endeavour. Fuel. 2018;211:891-897.
[10] Prabhakar B, Boehman, André L. Effect of common rail pressure on the relationship between efficiency and particulate matter emissions at NOx parity. SAE Technical Papers. 2012;1.
[11] Lou DM, Wu Y, Hu Z Y, et al. Experimental study on the influence of injection timing on combustion and emission of biodiesel engine based on mechanical mechanics. Advanced Materials Research. 2014;908(42):301-309.19
[12] Zhao G, Jia Q, Yao C, et al. Effect of per-injection strategy on combustion and emission characteristics of dual-fuel engines. Transactions of CSICE. 2020;38(01):19-26.
[13] Jia Q. The Influence of Diesel Injection Strategy on the Combustion and Emission Characteristics of Marine Duel Fuel Engine. Harbin: Harbin Engineering University. Master's Thesis. 2019.
[14] Wang L, Chen Z, Zhang T, et al. Effect of excess air/fuel ratio and methanol addition on the performance, emissions, and combustion characteristics of a natural gas/methanol dual-fuel engine. Fuel. 2019;255(NOV.1):115799.
[15] Lee CF, Pang Y, Wu H, et al. An optical investigation of substitution rates on natural gas/diesel dual-fuel combustion in a diesel engine. Applied Energy. 2020;261:114455.
[16] Ma C, Song E, Yao C, et al. Analysis of PPCI mode and multi-objective comprehensive optimization for a dual-fuel engine. Fuel. 2021;303(NOV.1):121296.
[17] Park S, Kim Y, Woo S, Lee K. Optimization and calibration strategy using design of experiment for a diesel engine. Applied Thermal Engineering. 2017;123:917-928.
[18] Ma C, Yao C, Song EZ, et al. Prediction and optimization of dual-fuel marine engine emissions and performance using combined ANN with PSO algorithms. International Journal of Engine Research. 2021;2.
[19] Cortes C, Vapnik VN. Support-vector networks. Machine Learning. 1995;20:273-297.
[20] Vapnik N. The Nature of Statistical Learning Theory. Springer. 1995.
[21] Shi C, Ji C, H Wang, et al. Comparative evaluation of intelligent regression algorithms for performance and emissions prediction of a hydrogen-enriched Wankel engine. Fuel. 2021;290:120005.
[22] Deb K, Sundar J, Bhaskara U, Chaudhuri S. Reference point based multi-objective optimization using evolutionary algorithms. International Journal of Computing Intelligent Research. 2006;2(3):273-286.
[23] Ben Said L, Bechikh S, Ghedira K. The r-Dominance: A new dominance relation for interactive evolutionary multicriteria decision making. IEEE Trans. Evol. Comput. 2010;14(5):801-818.
[24] Deb K, Jayavelmurugan S. Reference point based multi-objective optimization using evolutionary algorithms. International Journal of Computational Intelligence Research. 2006;2(3):635-642.